Thin-Film Recording Media I Hans Richter, Chairman

Origin of the orientation ratio in sputtered longitudinal media

B. G. Demczyk, J. N. Zhou, and G. Choe
MMC Technology, a Maxtor Company, 2001 Fortune Drive, San Jose, California 95131

E. Stach, E. C. Nelson, and U. Dahmen
National Center for Electron Microscopy, Lawrence Berkeley National Laboratory, 1 Cyclotron Road, Berkeley, California 94720

(Presented on 13 November 2002)

The surface morphology, thin film microstructure, and crystallography of sputtered longitudinal media were examined by atomic force and transmission electron microscopy. It was found that surface features along the texture lines in addition to the line density affect the measured orientation ratio. In addition, *c*-axis alignment along the texture line direction was established. These results point to magnetocrystalline anisotropy associated with the *c* axis as a major contributor to a high orientation ratio in these materials. © *2003 American Institute of Physics.*
[DOI: 10.1063/1.1558236]

I. INTRODUCTION

Magnetic hard disks for longitudinal data storage consist of a Co-based series of magnetic layers deposited on a mechanically textured NiP coated aluminum substrate. The precise origin of the in-plane magnetic anisotropy leading to the orientation ratio (OR) in these materials is yet to be established unambiguously, but its occurrence is critical to the design of even higher density media. Both theoretical[1,2] and experimental[3,4] studies have shown that an increased OR enhances recording performance, while thermally stabilizing the media. Potential sources of this anisotropy field include *c*-axis alignment within the plane of the disk,[5–8] stress,[4,7,9,10] and shape effects.[7,9] In this work, we have examined the surface morphology and film microstructure of these media in detail to gain a more fundamental understanding of the origin of their OR, and to suggest additional methods for its evaluation.

II. EXPERIMENT

Disk surface morphology was examined with a Digital Instruments Dimension 3000 atomic force microscope (AFM), operating in the intermittent contact (''tapping'') mode. To evaluate the microstructure and crystallography, transmission electron microscopy (TEM) was performed, using a Philips CM 200 field emission transmission electron microscope, operating at 200 kV accelerating voltage.

III. RESULTS AND DISCUSSION

Figure 1(a) shows a bright field TEM image of a region comprised primarily of NiP substrate material. One can clearly discern alternating light and dark bands of periodicity ~70 nm. These features are believed to represent the mechanical texturing lines imparted to the disk by a 0.1 μm diamond slurry treatment. The alternating light and dark contrast results from varying sample thickness in the electron beam direction.[11] The film composite consists of a Cr seedlayer, a CrMoX underlayer (X=grain boundary segregation enhancement element), a CoCrTa intermediate layer, and two CoCrPtB magnetic layers.

These texture lines can also be inferred from bright field images of the sputtered disk [Fig. 1(b)]. In general, grains along the ''sidewalls'' of the texture bands are not in a strong

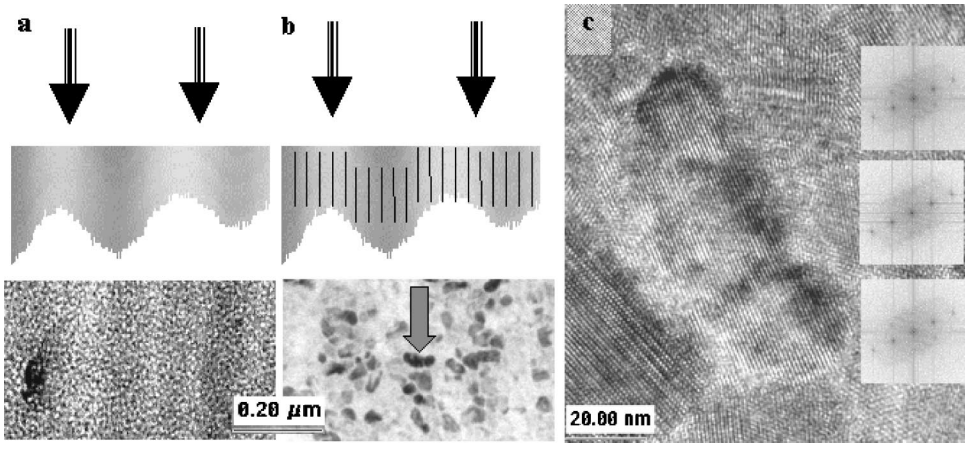

FIG. 1. Schematic depicting the origin of bands of light and dark contrast, as seen in TEM bright field images for: (a) amorphous and (b) crystalline regions of varying thickness. Arrows indicate the electron beam direction. Vertical lines in (b) represent atomic planes parallel to this direction. (c) High resolution (phase contrast) image of the grain cluster indicated by the arrow. Insets at right show FHT power spectra from the three adjoining grains ([1.10] zone axis).

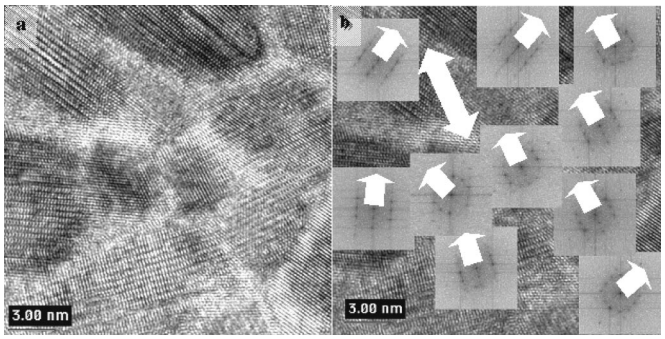

FIG. 2. (a). High resolution TEM image of grains around a mechanical texture line. (b). Same region with FHT patterns, *c*-axis direction (arrows), and texture line direction (double arrow) superimposed.

diffracting condition and do not appear in contrast. As shown, regions of dark contrast are observed in a wide size range, from well less than 0.02 μm to nearly 0.1 μm. As shown in Fig. 1(c), however, what may appear to be single grains in an amplitude contrast bright field image can actually be clusters of distinct, albeit closely oriented grains, as illustrated by the arrow in Fig. 1(b). This is established by the individual fast Hartley transforms (FHTs), shown alongside the grain cluster. These FHTs, which are analogous to local microdiffraction patterns, reveal a nearly identical [1.10] hcp zone axis pattern arising from each individual grain. The nearly identical orientation of these adjoining grains suggests that the entire ''cluster'' formed from the impingement of growth from adjacent nucleation sites and may act as a single magnetic entity. It is of interest to note that these clusters often form with their long axes perpendicular to the mechanical texture lines, which would preclude shape anisotropy as contributing to the observed magnetization parallel to the lines.

Alignment of the *c* axis along the texture lines is often invoked as a factor contributing to the observed in-plane anisotropy. This effect has been examined, using orientational dark field TEM imaging by several investigators. Guruswamy *et al.*[12] interpret enhanced dark field contrast along mechanical texture lines as indicative of *c*-axis alignment, while Nolan *et al.*[13] attribute such contrast to local topographic effects. For direct evidence, high resolution TEM was performed. Figure 2(a) depicts a collection of grains in the vicinity of a mechanical texture line, imaged at high resolution. In Fig. 2(b), individual [1.10] zone axis FHT power spectra are superposed and the direction of the *c* axis drawn in with an arrow. In this particular case, where the disk OR (Mrt) was 1.6, seven out of ten grains display *c*-axis alignment close to the texture line direction (double arrow). In fact, based solely on *c*-axis alignment, an OR of 1.6 would require ~30% of the grains to be ''perfectly aligned'' with the texture grooves. It has been found experimentally that media with lower measured OR values exhibit a lesser degree of alignment, often with out-of-plane *c*-axis components present.

The relationship of the surface morphology to the resulting OR has been investigated by Wong,[14] who reported that OR values increased more or less linearly with increasing roughness amplitude R_a. However, this parameter is not the only indicator of the surface profile. Figures 3(a) and 3(b) show high-resolution AFM images of a low (1.2) and a high (1.8) OR surface. In both cases, the R_a values are the same (0.4 nm). Close inspection, however, will reveal a higher ''line density'' (30 versus 15 per micron) for the OR=1.8 relative to the OR=1.2 surface. So, in this case, it appears that the line density is the relevant parameter. Figure 3(c) shows an OR=1.6 surface of identical roughness and line density to the OR=1.8 surface of Fig. 3(b). This ambiguity occurs increasingly in the present ''smooth'' (yet high OR) disk profile regime required to enable decreasing flying heights. Consequently, more detailed surface analysis is required. We have found the power spectral density (PSD) function (square of the Fourier transform) in the circumferential direction to provide additional insight into the details of the surface morphology along the mechanical texture line. Figure 4(a) compares the PSD curves for the high and low OR surfaces depicted in Figs. 3(a) and 3(b). In these plots, the *x* axis represents the wavelength (in microns) of circumferential features and the *y* axis, their corresponding contribution to the surface topography (the area under the curves corresponds to the surface roughness). A clear difference is noted in the 0.0075–0.05 μm wavelength regime (differences at longer wavelengths are due to the scan skew angle). This dimension corresponds to that of a single grain to a

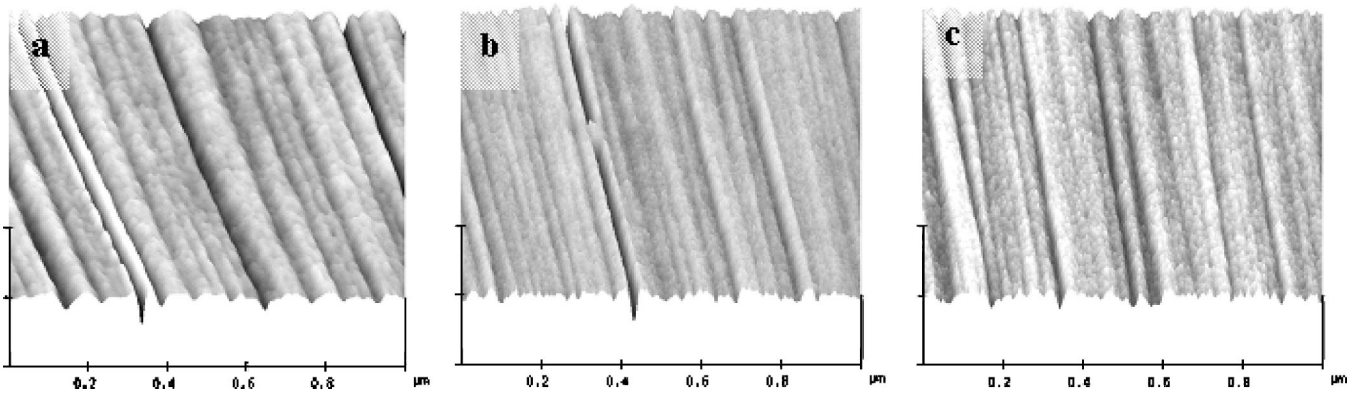

FIG. 3. High resolution atomic force micrographs of a: (a) low (OR=1.2), (b) high (OR=1.8), and (c) intermediate (OR=1.6) disk surfaces. Vertical height scale is 20 nm.

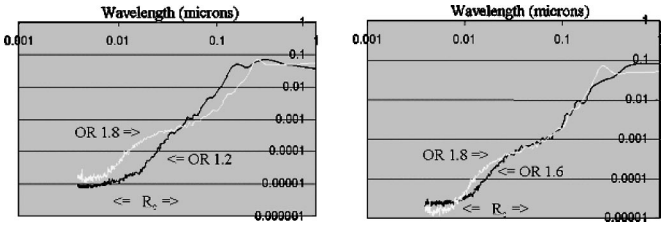

FIG. 4. (a) PSD function for two disk surfaces exhibiting highly different OR (1.2 dark, 1.8 light curve) values. (b) Corresponding curves for disk surfaces displaying closer OR (1.6 dark, 1.8 light curve) values.

cluster of, at most ten grains, as depicted in Fig. 1(b). In Fig. 4(b), the high (1.8) OR PSD curve is compared to that for an intermediate OR value (1.6) disk surface, depicted in Fig. 3(c). Even here, we observe a marked deviation of the curves in the above wavelength regime. Defining a ''circumferential roughness'' R_c as the area under the PSD curve between 0.0075 and 0.05 μm, we calculate values of 0.14, 0.12, and 0.08 nm for the OR=1.8, 1.6, and 1.2 surfaces, respectively.

Alignment of the *c* axes of Co-based alloy grains with the mechanical texture lines has been shown by x-ray diffraction[15,16] and TEM[17] to be related to distortion of the underlying Cr-based lattice structure, which relaxes anisotropically parallel and perpendicular to the mechanical texture lines.[10,18–20] In this way, pseudoepitaxial growth can be promoted. However, to this point, no explanation for the initial alignment of the Cr⟨110⟩ axes parallel to the texture lines (which is required for Co *c*-axis alignment) has been provided. Chung *et al.*[21] have described a conceptual model that relates the surface ''nanoroughness'' to the ''wettability'' of the Cr nuclei on the disk surface. In this model, a high roughness leads to a less wettable surface. Since the lowest energy planes of the Cr bcc lattice are the closest-packed ones, (110), a high wetting condition (lower roughness) would promote (110) growth parallel to the local surface.[22] In a high roughness condition, (002) growth would be obtained. The scale of the roughness is important, however. In Fig. 5, the Cr growth scenario on a relatively smooth disk surface with a high circumferential roughness is depicted, schematically. Looking only along the circumferential direction (i.e., paying attention to R_a or ''line density'' alone), the disk surface is relatively flat ($R_a/L=0.005$, where R_a is the two-dimensional surface roughness amplitude and L is the texture line wavelength). Viewed radially, however, the surface appears much rougher ($R_c/R_a=0.42$, where R_c is the circumferential roughness, defined as above). Therefore, to minimize the surface free energy, a high R_c value tends to ''lock in'' the orientation of the Cr grains, with (100) growth (and consequently ⟨110⟩ alignment) parallel to the texture groove. We have found a good correlation of this parameter and measured OR values on ''smooth'' disk surfaces.

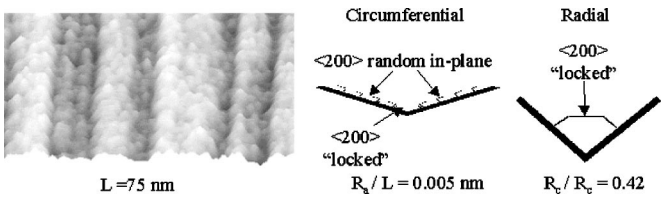

FIG. 5. Schematic growth model of Cr on the disk surface at left, viewed circumferentially and radially. L is the texture wavelength, R_a, R_c are the two-dimensional roughness amplitude and circumferential roughness, respectively.

IV. CONCLUSIONS

TEM results show grains in textured longitudinal media to grow as correlated clusters, often with their long dimension orthogonal to the mechanical texture line. Evidence was presented for crystallographic (*c* axis) alignment along texture lines. These results suggest that the high orientation ratios observed in these media may result from the magnetocrystalline anisotropy associated with *c*-axis alignment along the texture lines. This alignment is though to arise via pseudoepitaxial growth of Co-based magnetic grains onto the Cr underlayer which, itself, tends to align its ⟨110⟩ parallel to the mechanical texture lines to minimize the surface free energy. Circumferential roughness has been found to be a useful gauge of this tendency, especially on smooth disk surfaces. The foregoing suggests that achieving a large circumferential roughness is a key parameter in attaining high OR disks on smooth surfaces.

[1] J. P. Wang, C. H. Hee, and T. C. Cheong, IEEE Trans. Magn. **36**, 3199 (2000).
[2] J. V. Ek and M. Plumer, in *The Physics of Ultra High Density Recording*, edited by M. Plumer (Springer, New York, 2001), p. 29.
[3] G. Choe *et al.*, IEEE Trans Magn. (in press).
[4] M. Yu, G. Choe and K. E. Johnson, J. Appl. Phys. **91**, 7071 (2002).
[5] G. Khanna, B. M. Clemens, H. Zhou, and H. N. Bertram, IEEE Trans. Magn. **37**, 1468 (2001).
[6] H. Kataoka, J. A. Bain, S. Brennan, and B. M. Clemens, J. Appl. Phys. **73**, 7591 (1993).
[7] K. E. Johnson, M. Mirzamaani, and M. E. Doerner, IEEE Trans. Magn. **31**, 2721 (1995).
[8] P. W. Wang, J. Appl. Phys. **73**, 6692 (1993).
[9] M. R. Kim, S. Guruswamy, and K. E. Johnson, J. Appl. Phys. **74**, 4643 (1993).
[10] C. A. Ross, M. E. Schabes, R. Ranjan, G. Bertero, and T. Chen, J. Appl. Phys. **79**, 5342 (1996).
[11] P. Hirsch, A. Howie, R. B. Nicholson, D. W. Pashley, and M. J. Whelan, *Electron Microscopy of Thin Crystals* (Krieger, Malabar, FL, 1977), p. 159.
[12] S. Guruswamy, J. E. Shield, and M. Tarakei, Scr. Mater. **39**, 647 (1998).
[13] T. P. Nolan, R. Sinclair, R. Ranjan, and T. Yamashita, J. Appl. Phys. **73**, 5117 (1993).
[14] B. Wong (unpublished).
[15] J. A. Bain, B. M. Clemens, S. M. Brennan, and H. Kataoka, IEEE Trans. Magn. **29**, 300 (1993).
[16] T. Hirose, T. Teranishi, M. Ohsawa, A. Ueda, O. Ishiwata, T. Ataka, K. Ozawa, S. Kamiya, and A. Iida, IEEE Trans. Magn. **33**, 2971 (1997).
[17] A. Ajan, B. R. Acharya, E. N. Abarra, and I. Okamoto, IEEE Trans. Magn. **37**, 1508 (2001).
[18] A. Kawamoto and F. Hikami, J. Appl. Phys. **69**, 5151 (1991).
[19] R. Murao, K. Takahashi, C. Okuyama, A. Kikuchi, Y. Kitamoto, and S. Ishida, Jpn. J. Appl. Phys., Part 1 **25**, 615 (2001).
[20] E. Marinero, T. Rieth, M. F. Toney, and B. York, J. Appl. Phys. (in press).
[21] J. J. K. Chang, Q. Chen, G. L. Chen, and R. Sinclair, J. Appl. Phys. **81**, 3943 (1997).
[22] Y. C. Feng, D. E. Laughlin, and D. M. Lambeth, J. Appl. Phys. **76**, 7311 (1994).